

Eastern Kentucky University

Encompass

Geosciences Undergraduate Theses

Geosciences

Spring 5-2019

Nutrient Export at Meadowbrook Farm, Madison County, Kentucky: Steps Toward Improving Local and Regional Water Quality

Ryan M. Penn
Eastern Kentucky University

Follow this and additional works at: https://encompass.eku.edu/geo_undergradtheses

Recommended Citation

Penn, Ryan M., "Nutrient Export at Meadowbrook Farm, Madison County, Kentucky: Steps Toward Improving Local and Regional Water Quality" (2019). *Geosciences Undergraduate Theses*. 9. https://encompass.eku.edu/geo_undergradtheses/9

This Restricted Access Thesis is brought to you for free and open access by the Geosciences at Encompass. It has been accepted for inclusion in Geosciences Undergraduate Theses by an authorized administrator of Encompass. For more information, please contact Linda.Sizemore@eku.edu.

**NUTRIENT EXPORT AT MEADOWBROOK FARM,
MADISON COUNTY, KENTUCKY:
STEPS TOWARD IMPROVING LOCAL AND REGIONAL WATER QUALITY**

**By
RYAN M. PENN**

**Undergraduate Thesis
Submitted to Walter S. Borowski
Department of Geosciences
Eastern Kentucky University
10 May 2019**

ACKNOWLEDGMENTS

I would like to thank Meadowbrook Farm personnel Justin McKinney (Director) and Chad Powers (Manager) for their continued help and access to the Farm. Dr. Jonathan M. Malzone helped in calculating nutrient export values using cubic spline functions and *Microsoft Excel*. The ECU University Research Committee, Sponsored Programs, University Fellows, and Undergraduate Research and Creative Endeavors provided funds for this research.

ABSTRACT

Excess nutrient levels in surface water continues to be one of the leading causes of water degradation in the United States today. Excess nutrients usually are sourced from agricultural-practices in the form of non-point-source contamination. Both large- and small-scale farming practices can result in excess nutrients contaminating local water ways, mostly injected during and shortly after rain events. The most prevalent nutrients in these cases include dissolved and solid forms of nitrogen and phosphorus.

In Madison County, Kentucky, we investigate the nutrient export from Meadowbrook Farm, located within the Muddy Creek watershed, which flows into the Kentucky River and ultimately into the Mississippi river drainage basin. This small-scale farm, owned and operated by Eastern Kentucky University, raises typical crops and livestock. We quantify the nutrient export from the Farm in the form of dissolved nitrogen (ammonium, NH_4^+ ; nitrate, NO_3^-), dissolved phosphorus (orthophosphate, PO_4^{3-}), and total phosphorus (ΣP).

We sampled water flowing over an instrumented weir, situated within the Farm's Big Runoff Channel (BRC), during six different storm events in the 2018 field season. We determined nutrient concentrations during storms coupled with respective discharge measurements. Then, we used a cubic spline function embedded within *Microsoft Excel* that interpolated between data points to produce a continuous curve for each nutrient species and discharge. The area under these curves generates total water volume and nutrient export values for each storm event. The largest storm event (6-7 July) exported 4.1 kg of P- PO_4 ; 11.3 kg of total phosphorus; 3.3 kg of N- NH_4 ; and 1.7 kg of N- NO_3 [5 kg N].

An approximate linear relationship between total storm water volume and P- PO_4 , ΣP , and N- NO_3 is observed. However, these relationships are not robust enough to reliably estimate

nutrient transport for any rainfall event from discharge data alone. The next step is to test if better relationships occur between nutrient export and rainfall intensity, rain event frequency, or other possible parameters. The overall aim is to estimate annual nutrient export with confidence in order to: (1) test the efficacy of mediation efforts to on the Farm; and (2) to compare annual nutrient export values to those of other studies.

TABLE OF CONTENTS

I.	INTRODUCTION.....	1
II.	METHODS.....	5
	Study Area.....	5
	Sampling.....	6
	Nutrient Analyses.....	7
	Export Calculations.....	10
III.	RESULTS.....	13
IV.	DISCUSSION.....	17
	Base Flow versus Storm Nutrient Export.....	17
	Relationship Between Flow Volume and Nutrient Export.....	19
	Next Steps.....	21
V.	SUMMARY.....	23
VI.	REFERENCES.....	24
VII.	APPENDIX.....	28

LIST OF TABLES

1. Summary of total water volume (L) and nutrient export (kg) for each measured storm event.....	16
2. Statistical parameters of baseflow concentration.....	17

LIST OF FIGURES

1. Map of Meadowbrook Farm.....	5
2. Characteristics of the BRC watershed.....	6
3. Scatter plots showing the first storm peak of tropical storm Cindy.....	11
4. Reimann sum method of integration.....	12
5. Rainfall and discharge during the field season of 2018.....	13
6. Flow and concentration of dissolved ammonium over the duration of the 30-31 May 2018 storm event.....	14
7. Flow and concentration for each nutrient over duration of the 30-31 May 2018 storm event.....	15
8. Box-and-whisker plot of concentration during the field seasons of 2016, 2017, and 2018.....	18
9. Comparing nutrient export of each nutrient species during baseflow and storm events.....	18
10. Nutrient export values for each nutrient species versus total water volume.....	20
11. Three-dimensional plot of NH ₄ export.....	21
A1. Flow and concentration for each 2018 storm event.....	29

INTRODUCTION

Water is one of the planet's most invaluable resources: a necessity for all life on Earth. Especially since the industrial age and the onset of large-scale farming practices, water contamination has been a widespread and lingering problem (Smith et al., 1999). Before the 21st century, most water pollution in the United States came from industrial processes in the absence of environmental standards, usually from single, easily-identifiable sources (Neary et al., 1989). This is also known as point-source pollution or contamination. With the passage and enforcement of the Clean Water Act in 1972, much of point-source pollution in the United States has been mitigated (Hornbeek, 2011).

Today, most water contamination stems from non-point-source pollution (Baker et al., 1992). In these cases, contamination occurs from many small sources whose individual contaminant contributions aggregate to create large contamination problems. It is typically difficult to measure, access, and mitigate contamination from these various and dispersed sources (Moltz et al., 2011). One typical type of non-point-source pollution arises as excess nutrient export of solid and dissolved forms of nitrogen and phosphorus into natural waterways. Whereas nutrients are essential for aquatic organisms and ecosystem sustainability, over-enrichment can have detrimental effects on these systems (U.S. National Research Council, 2000).

Nutrient loading of aquatic ecosystems occurs through many varying processes, including atmospheric, fluvial, and groundwater inputs into lakes, streams, and coastal areas (Smith et al., 1999). The largest inputs originate from anthropogenic activities, such as agricultural and urban runoff (Carpenter et al., 1998). It is well documented that increasing human population has a direct relationship with increasing nitrogen and phosphorus export, typically due to increasing

use coupled with lack of proper resource management (Smith et al., 1999; Stokal et al., 2016; U.S. National Research Council, 2000).

Excess nutrient supply can ultimately lead to eutrophication, an oversupply of organic matter to an ecosystem (Pinckney et al., 2001). Eutrophication plagues many fresh water systems throughout the United States and much of the developed world (Carpenter et al., 1998; Smith et al., 1999; Jiake et al., 2018). In many of these systems, primary productivity is directly influenced by nutrient supply. Nitrogen and phosphorus over-enrichment most commonly leads to the growth of harmful phytoplankton (toxic algae blooms) by increasing the primary productivity in these ecosystems (U.S. National Research Council, 2000).

Along with toxic algae blooms, eutrophication adversely affects ecosystems in other ways, such as increased biomass of aquatic weeds, damaging or destroying coral reef communities, decreasing water transparency, limiting use of human water resources, and many others (Carpenter et al., 1999; Pinckney et al., 2001; U.S. National Research Council, 2000). One of the primary consequences of eutrophication is the significant decrease in dissolved oxygen, which is used up by microbial decomposition of excess phytoplankton and aquatic plant tissue (Diaz and Rosenberg, 2008). Dissolved oxygen can ultimately lead to hypoxia and subsequent benthic dead zones (Dodds, 2006).

Dead zones are characterized by mass mortality of benthic fauna and major shifts in in community structure and ecosystem dynamics (Dodds, 2006). Globally, dead zones have approximately doubled since the 1960's, developing in areas such as the Baltic, Kattegat, Black Sea, East China Sea, and Chesapeake Bay (Diaz and Rosenberg, 2008). One of the largest dead zones in the world is located within the northern Gulf of Mexico, characterized by estuarine and coastal hypoxia (Rabalais et al., 2002). Seventy percent of the nutrients that enter the Gulf

originate within the Mississippi River drainage basin (Dodds, 2006), which is largely made up of farmland and pasture.

Nutrient export varies among watersheds with regard primarily to size and land use (Jordan et al., 1997). Agricultural areas overwhelmingly contribute more nitrogen and phosphorus than other considered land uses such as forest and residential (Cooke and Prepas, 1998; Carpenter et al., 1998; Dubrovsky et al., 2010). Export values differ further among agricultural practices such as the cultivation of row crops (corn, soy, and wheat), livestock, and pasture (Arbuckle and Downing, 2001; Jordan et al, 1997). The highest nitrogen exporting practices are observed to originate from cultivating row crops, while the highest phosphorus originates from raising livestock.

Nitrogen is most typically applied to croplands in the form of fertilizer or animal manure, for which regulatory standards are lacking (Smith et al., 1999). This sometimes results in an oversupply of nitrogen, as more is applied than is needed for plant growth. Phosphorus application suffers in a similar manner, as excess is applied to farmland and urban areas when soils already contain adequate levels (Carpenter et al., 1998; Smith et al., 1999). These issues, coupled with nutrient inputs from livestock manure, lead to higher nutrient export.

Mitigating water degradation caused by excess nutrients first involves determining a suitable method to model nutrient loads (Smith et al., 1999). Public opinion and societal objectives are also a major factor in what issues are addressed and what policies are adopted (U.S. National Research Council, 2000). For agricultural areas, the focus is usually the adoption of better management practices such as improved regulations on fertilizer applications to farmland.

Another important consideration with regard to agricultural watersheds is the impact of riparian zones in lessening nutrient export (Cooke and Prepas, 1998; Vanni et al., 2001). Riparian zones are aquatic, as well as boundaries between aquatic and terrestrial ecosystems, that usually consist of dense vegetation (Blinn and Kilgore, 2001). Riparian vegetation plays an important role in biofiltration, the trapping of dissolved nutrients and nutrient-rich sediment before reaching waterways (Allaire et al., 2015). Riparian buffers can be utilized in agricultural areas and have been found to significantly decrease nutrient export (Allaire et al., 2015; Gharabagh et al., 2006; Zhang et al., 2010).

The first goal of this research is to quantify the amount of nutrient export from Meadowbrook Farm located in Madison County, Kentucky. These baseline values will serve as a benchmark with which to evaluate future remediation measures that will attempt to decrease nutrient export from the Farm. If export is indeed lowered, these remediation methods can be used in other agricultural areas locally, regionally and globally to improve overall water quality with regard to nutrient load and eutrophication. We specifically measure export of dissolved nitrogen (ammonium, NH_4^+ ; nitrate, NO_3^-), dissolved phosphorus (orthophosphate, PO_4^{3-}), and Total Phosphorus (ΣP) that is discharged from a small, intermittent stream that drains into Muddy Creek, a tributary to the Kentucky River, part of the Mississippi River drainage basin.

METHODS

Study area

We investigated the export of nutrients from a portion of Meadowbrook Farm, Madison County, Kentucky into Muddy Creek (Figure 1). Owned and operated by Eastern Kentucky University, the Farm spans 720 acres (~2.9 km²) of land, used in raising corn, soybeans, and livestock including mainly dairy and beef cattle. Nutrient sources include fertilizer used for crop areas, livestock manure that is applied to crop land and pasture, and cow manure that occurs in pasture and concentrated at the dairy complex.

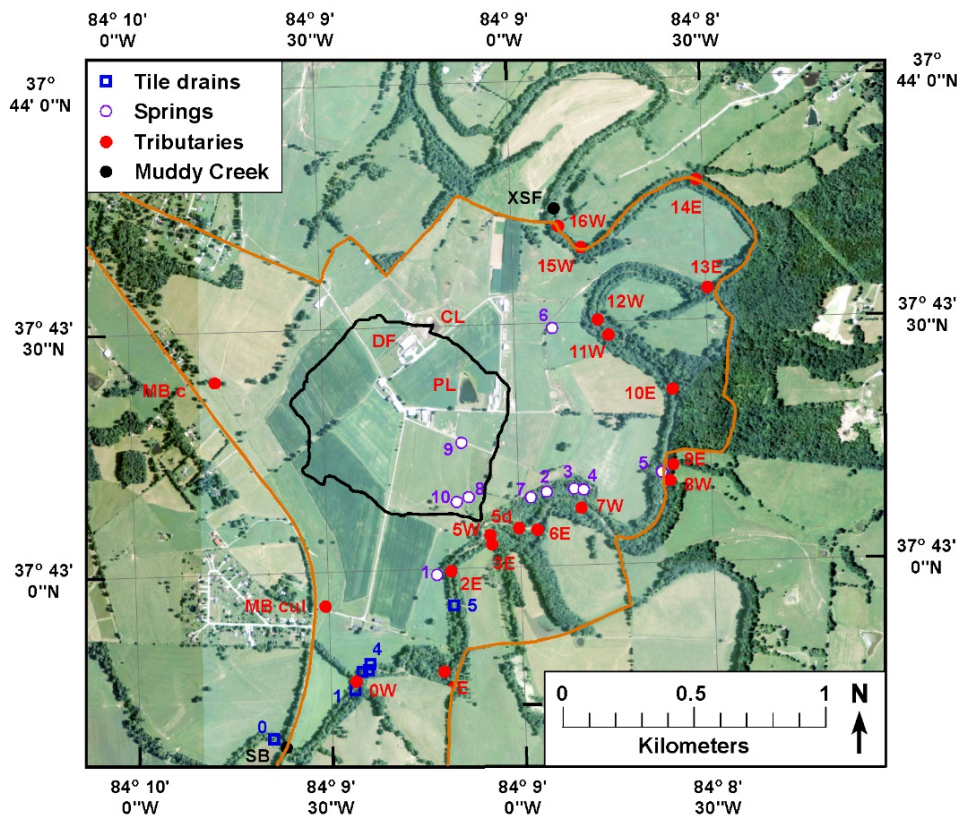


Figure 1: Map of Meadowbrook Farm and its relationship to Muddy Creek in Madison County, Kentucky. The outline of the Farm is shown in orange. Muddy Creek flows from south to north on the eastern edge of the Farm. Sampling stations are shown with various symbols and provide information about background or base flow nutrient concentration. The watershed of the Big Runoff Channel (BRC) is shown by the black polygon. Note that cropland, pasture, the dairy complex (DF), and of the lagoons that hold cow (CL) and pig (PL) waste are within the BRC watershed. The sampling weir of this study is located approximately 20 meters upstream of station 5W.

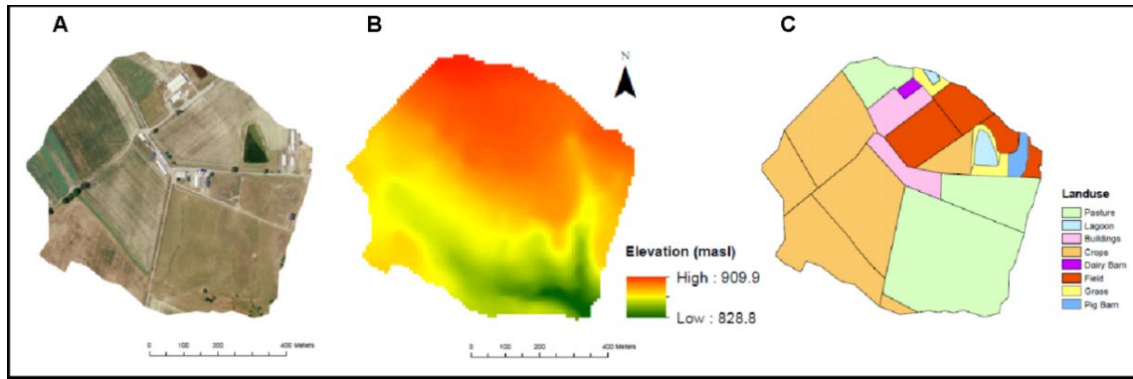


Figure 2: Characteristics of the BRC watershed. A shows satellite imagery, B shows topography, and C shows landuse. All maps after Kelley et al. (2017).

The Farm is drained by two main creeks, one of which is the Big Runoff Channel (BRC) (Figure 1, 2) that flows directly into Muddy Creek. The BRC watershed drains a representative portion of the farm that includes crops, the dairy complex, and pasture land supporting beef cattle. The BRC is a low relief and intermittent stream, which is active during certain portions of the year, mainly during and after rain events. These rain events export most of the nutrients originating from the Farm. Our strategy is to systematically sample BRC waters during storm events to estimate nutrient export from this representative portion of the Farm

Sampling

Background Sampling

To establish nutrient concentration during non-rain events, sampling was completed within the BRC, other tributaries entering Muddy Creek, and Muddy Creek in the field seasons of 2016, 2017, and 2018 (Buskirk et al., 2017; Evans et al., 2017; Echevarria et al., 2017). 60 mL syringes were used to collect water samples. Samples were then forced through a 0.45 μ m syringe filter, acidified to a pH of 2.0 using H₂SO₄ for preservation, bottled, and typically measured within a day or two of sampling.

Weir Sampling

Situated in the BRC is an instrumented weir. The weir is equipped with a data logger that monitors the water level behind the dam. When water flows through the V-shaped notch in the weir, the discharge (m^3/sec or L/min) can be calculated using recorded water levels. These data are recorded dynamically dependent on flow rate with measurement intervals ranging from 10 minutes to fractions of a second.

We also took water samples during storm events at the weir using an autosampler. Depending on the situation, the autosampler took samples at intervals ranging from 10 minutes to 2 hours. Dependent on the amount of rainfall and the length of any rain event, the main portion of storms usually encompasses about 4 to 8 hours followed by gradual decrease in discharge. During early portions of the storm, we typically sample at smaller time intervals. As discharge gradually decreases after the core period of the rain event, larger sampling intervals are adequate to measure nutrient export.

The water samples were used to measure the concentration of nutrients: dissolved ammonium (NH_4^+); dissolved nitrate (NO_3^-); dissolved orthophosphate (PO_4^{3-}), and total phosphorus (ΣP), which occurs as dissolved, absorbed, and complexed phosphorus.

Nutrient Analyses

Ammonium analysis

For ammonium analyses, we used the sodium hypochlorite method of Solorzano (1969) as modified by Gieskes et al. (1991). This method involves the diazotization of phenol and oxidation by chlorox to achieve a blue shade. The method measures both ammonium (NH_4^+) and ammonia (NH_3), but at natural pH the preponderant species is ammonium.

We prepared a standard stock solution from ammonium chloride (NH_4Cl) using 18.2 M Ω deionized water. The stock solution had a concentration of 100.3 mg/L (or parts per million, ppm) N- NH_4 , 129.2 mg/L NH_4 . Serial dilutions of the standard stock solution produced standards ranging from 0 to 12.5 mg/L N- NH_4 .

The sodium hypochlorite method uses phenol-ethyl alcohol solution, sodium nitroprusside, alkaline solution (sodium citrate and NaOH), oxidizing solution (Chlorox), and standards or sample. The resultant mixture develops varying shades of blue that are proportional to ammonium concentration. We measured standards and samples at 640 nm using a UV-VIS spectrophotometer. Standard curves of concentration vs. absorbance had linear correlation coefficients (r^2 values) of typically 0.997 to 0.999. Ammonium measurements were then calibrated to a reference standard (Ricca; 2.9 mg/L NH_4 , ~1.9 mg/L N- NH_4). Repeatability experiments reveal typical accuracy and precision of ~0.1 mg/L.

Nitrate analysis

We used ion-exchange chromatography (IC) to measure N- NO_3 using a Metrohm ion chromatograph. The standard stock solution was made from potassium nitrate (KNO_3) using 18.2 M Ω deionized water at a concentration of 16.9 mg/L N- NO_3 (75.2 mg/L NO_3). Serial dilutions of the standard stock solution produced standards ranging from 0 to 8.5 mg/L N- NO_3 . Standard curves had a typical r^2 value of 0.9999.

Nitrate measurements via IC were calibrated to a reference standard (Sigma-Aldrich, Multi-Anion Standard 1; 20 mg/L NO_3 , ~4.5 mg/L N- NO_3). Typical accuracy and precision approaches 0.01 mg/L, but we report concentration to the nearest 0.1 mg/L.

Orthophosphate analysis

We colorimetrically measure the concentration of dissolved orthophosphate (PO_4^{3-}) using the ascorbic acid method (Strickland and Parsons, 1968; modified by Gieskes et al., 1991). The standard stock solution was made from solid potassium phosphate (K_2HPO_4) using 18.2 M Ω deionized water to produce a concentration of 42.1 mg/L P- PO_4 (129.1 mg/L PO_4). Serial dilutions produced standards ranging from 0.0 to 12.5 mg/L P- PO_4 .

Both standards and samples were measured at 885 nm using a UV-VIS spectrophotometer. Standard curves typically had r^2 values of 0.997 to 0.999. Phosphate measurements were calibrated to a reference standard (Ricca; 5.0 mg/L PO_4 , ~1.6 mg/L P- PO_4). Repeatability experiments reveal typical accuracy and precision of ~0.1 mg/L.

Total phosphorus analysis

Measurements of Total Phosphorus (ΣP) include phosphorus within dissolved orthophosphate (PO_4^{3-}), phosphorus absorbed onto suspended sediment particles, organic particles, and metal-phosphate complexes (Guang and Bierma, 2018). We did a digestion procedure outlined by Doolittle (2014) that liberates phosphorus from the sources above and converts it to orthophosphate. Then we measured dissolved orthophosphate using the ascorbic acid method as above (Strickland and Parsons, 1968; modified by Gieskes et al., 1991).

The standard stock solution was prepared from solid potassium phosphate (K_2HPO_4) with a concentration of 292.8 mg/L P. Serial dilutions produced standards ranging from 0 to 14.9 mg/L P. For the digestion procedure, we filled digestion vessels to 50 ml and then added 1.0 ml of 11 N sulfuric acid (H_2SO_4) to release bound phosphate into solution. To convert free phosphate to orthophosphate, 1.0 ml of ammonium persulfate ($(\text{NH}_4)_2\text{S}_2\text{O}_8$) was used. Digestion

was completed using a *HotBlock* apparatus (Environmental Express) heated to ~125°C with samples simmering for at least 4 hours, which typically evaporated approximately 30 to 40 ml of the solution (Doolittle, 2014).

To prepare for measurements, we added phenolphthalein indicator solution and titrated with NaOH to bring the pH to 7. Then H₂SO₄ was added to return solutions from pink to clear, indicating slightly acidic conditions. 18.2 MΩ deionized water was added to bring the solutions up to a volume of 50 ml. Then 8 ml of mixed reagent – ammonium molybdate, sulfuric acid, ascorbic acid, potassium antimonyl – was added to each solution. Both standards and samples were measured at 885 nm using a UV-VIS spectrophotometer as above. Standard curves typically had r^2 values of 0.997 to 0.999. Total Phosphorus values were calibrated to a reference standard (Ricca).

Export Calculations

To best calculate nutrient export, water samples must be caught immediately before the rain event, throughout the entire rain event, and during or after flow equilibration after the rain event. We sampled 3 such rain events in 2017 (4-5 May; 13-14 June; and 22-25 June; Winter et al., 2018) and 6 events in 2018 (30-31 May; 31 May-1 June; 11-12 June; 12-14 June; 20 June; and 6-7 July).

As an example, Figure 3 shows the rain event of 22-23 June 2017, during the leading portion of tropical storm Cindy. Water level data from the weir are converted to discharge and are shown as a nearly continuous string of data points. In contrast, nutrient data are only available every 30 minutes as autosampler samples.

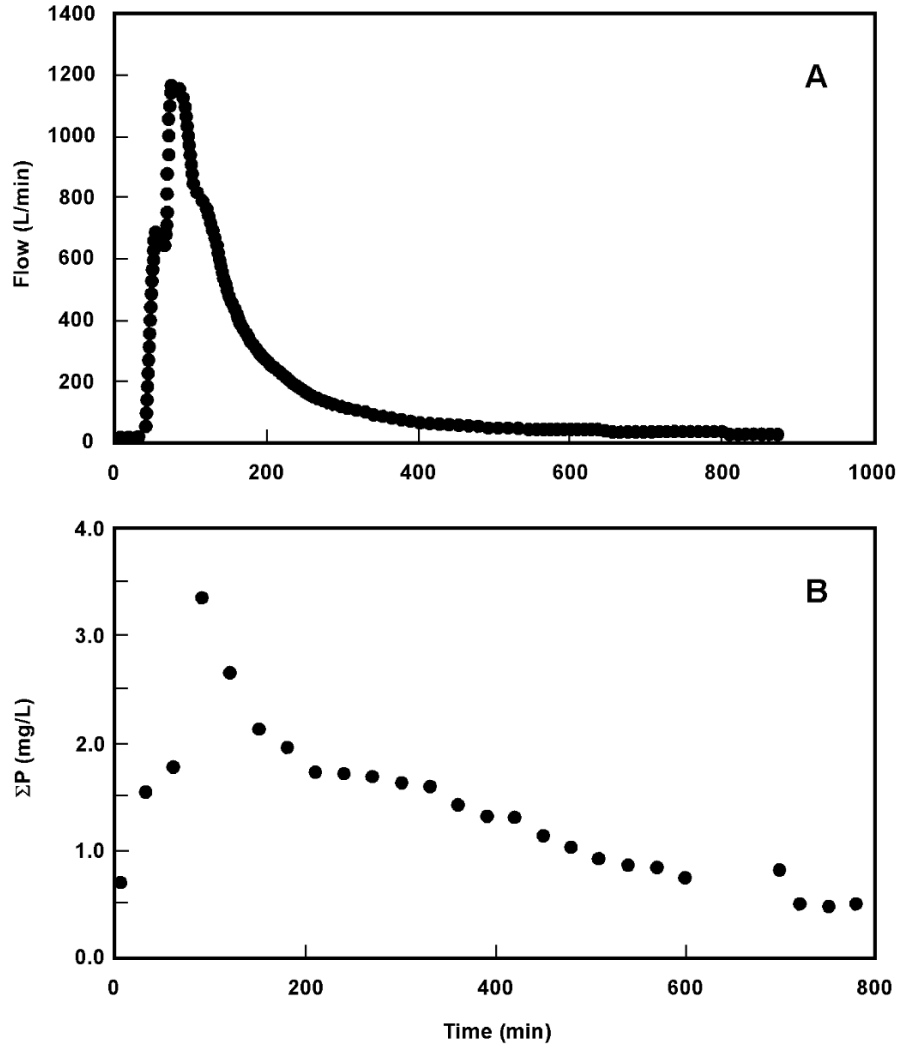


Figure 3: Scatter plots showing the first storm peak of tropical storm Cindy during 22-23 June 2018. A. Flow (L/min) vs time (min); B. Total phosphate (mg/L) vs storm time (min).

In order to calculate flow volume and nutrient mass per unit time, we need to integrate under the curve of flow versus time and of nutrient concentration versus time. With these methods, there are two inherent problems: 1) the curves do not follow mathematical functions; and 2) the time increment between data points for flow and concentration are very different.

To solve these problems, we use a cubic spline function to interpolate between data points and form a smooth curve. The cubic spline function is imbedded in *Microsoft Excel* and is

available from *SRSI Software, LLC*. Both the discharge and concentration data are interpolated into 0.5-minute increments. Multiplying discharge and concentration:

$$\frac{L}{min} \times \frac{mg}{L} = \frac{mg}{min}$$

yields the mass of the nutrient per unit time. Mass of the nutrient multiplied by each 0.5-minute time increment:

$$\frac{mg}{min} \times 0.5 min = mg$$

gives the mass of the nutrient in that time interval. Using the Reimann sum method of integration over the entire rain event (Figure 4) yields the total export amount in mass units of milligrams (mg). We then convert mg to kilograms (kg):

$$1 mg \times \frac{1 g}{1000 mg} \times \frac{1 kg}{1000 g}.$$

Total water volume is calculated similarly; discharge for each time increment multiplied by 0.5 minutes yields volume in liters (L). Summation of all time increments gives the total amount of water in the rain event.

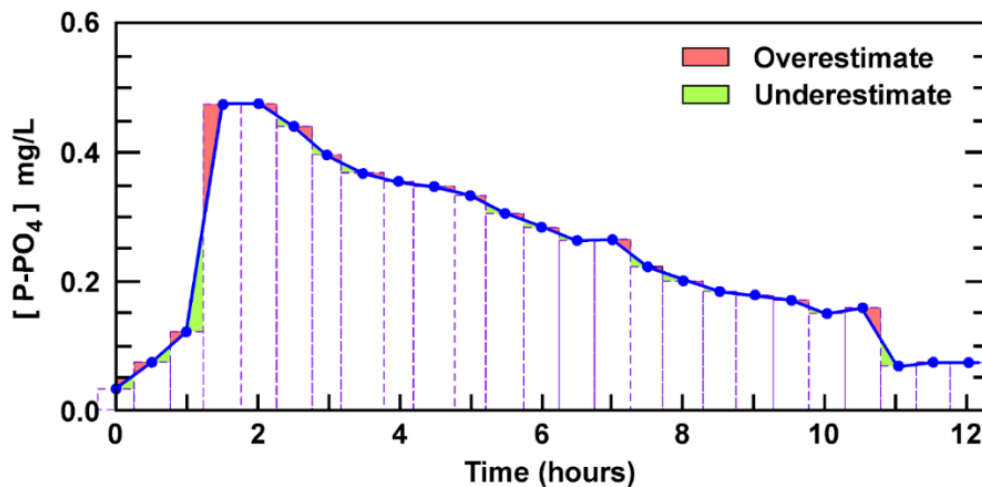


Figure 4: Graph showing the Reimann sum method of integration of phosphate over a sampling interval of 30 minutes. Graph after Winter et al. (2018).

RESULTS

We successfully recorded and analyzed 6 storm events in 2018 noting total rainfall (Kentucky Mesonet), measuring discharge, and estimating total nutrient export (Figure 5). We observed a variety of rainfall conditions throughout the field season of 2018. Our measurements were concentrated in June and July, when we generally recorded small to medium storm events.

As an example, discharge and nutrient data are shown for 30-31 May 2018 below (Figure 6). Again, note that the sampling intervals for hydrograph data versus nutrient data are very different. Discharge data has much higher resolution over the time interval of the storm, whereas nutrient measurements are lower resolution with samples taken every 15, 30, 60, or 120 minutes. Note that applying the cubic spline function to each set produces a smooth curve that can be integrated using the Reimann sum method with a time resolution of 0.5 minutes (Figure 6.B)

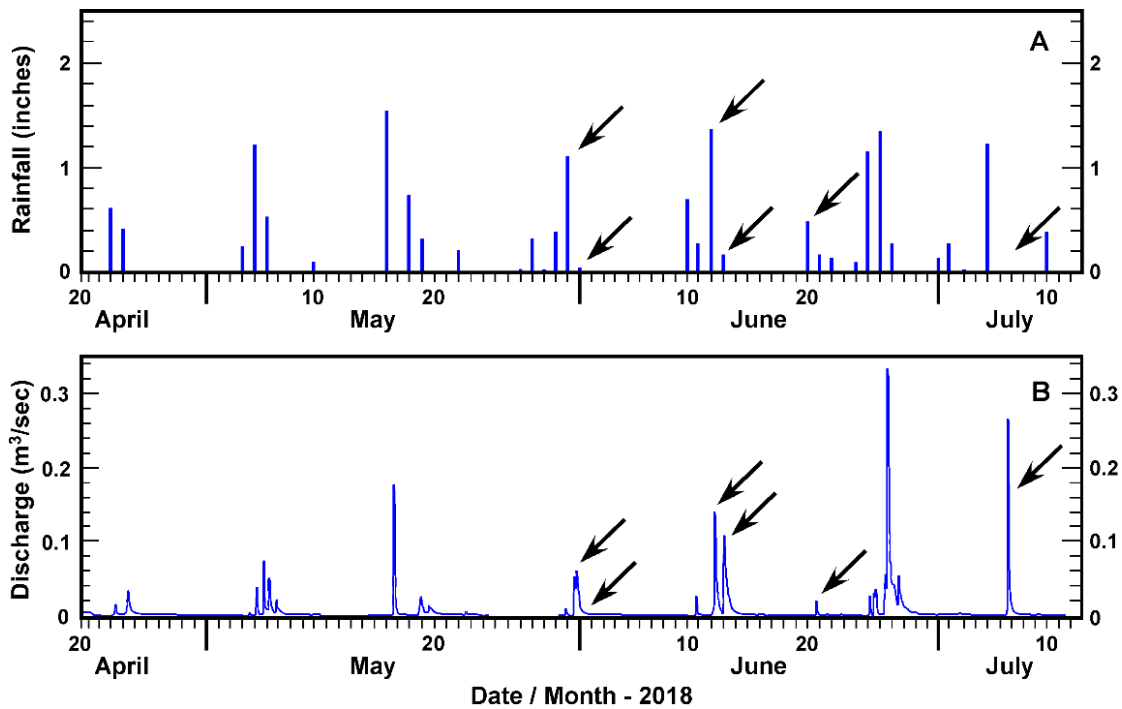


Figure 5: A. Rainfall occurring during the field season of 2018 from the Kentucky Mesonet Station located within the BRC watershed. B. Hydrograph showing discharge (m^3/sec) during the same time period. Nutrient export was calculated for the events shown with arrows.

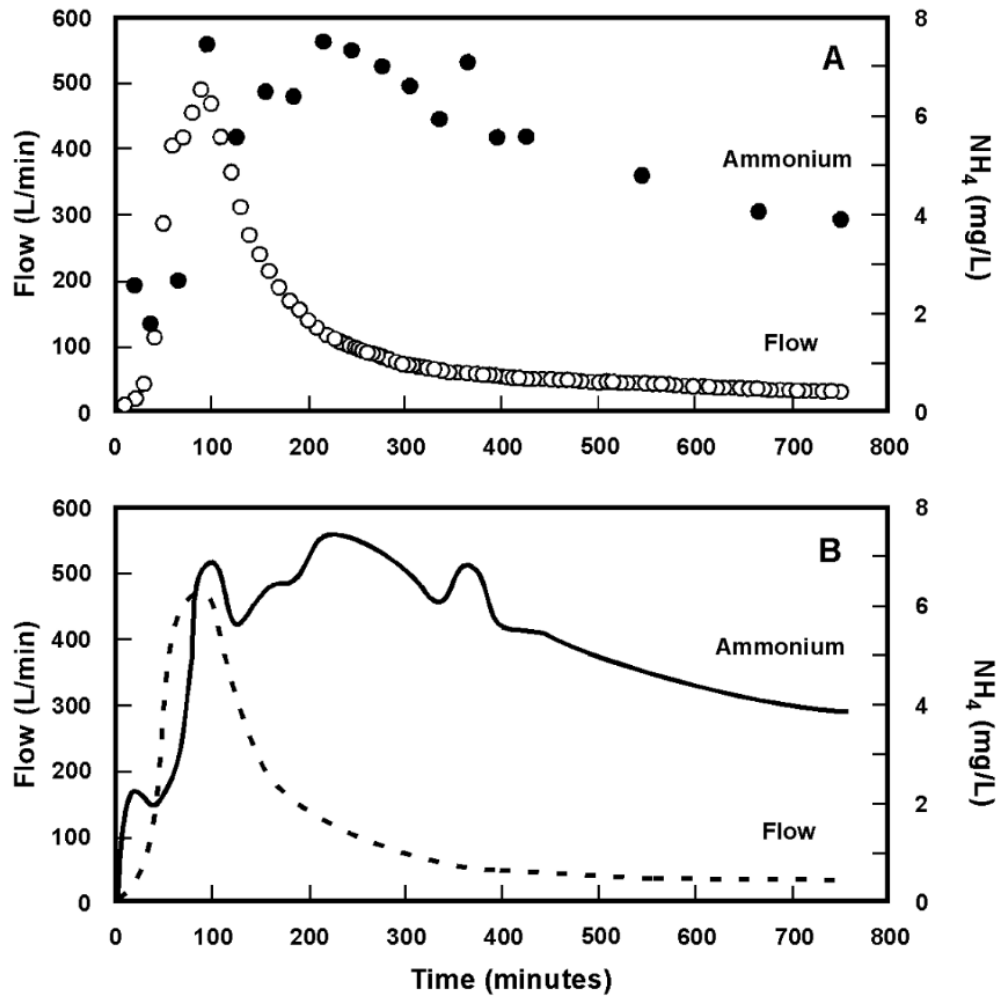


Figure 6: A. Graph showing flow (L/min) and concentration of nitrogen as dissolved ammonium (NH_4 ; mg/L) over the duration of the 30-31 May 2018 storm event showing discrete data points. B. Same plot as A, showing the application of the cubic spline function to each data set.

The nutrient concentration and total volume values for the 30-31 May storm are charted below (Figure 7); all other storm plots can be found in the Appendix. Peak nutrient values occur at, or shortly after, peak discharge in each case (Buskirk et al., 2018). Interestingly, N- NH_4 export values were the highest of all nutrients in this case. For all dissolved nutrients, concentration remained high even after discharge had equilibrated to baseline values. Total phosphorus values returned to baseline concentrations most quickly, closely coinciding with the discharge pattern.

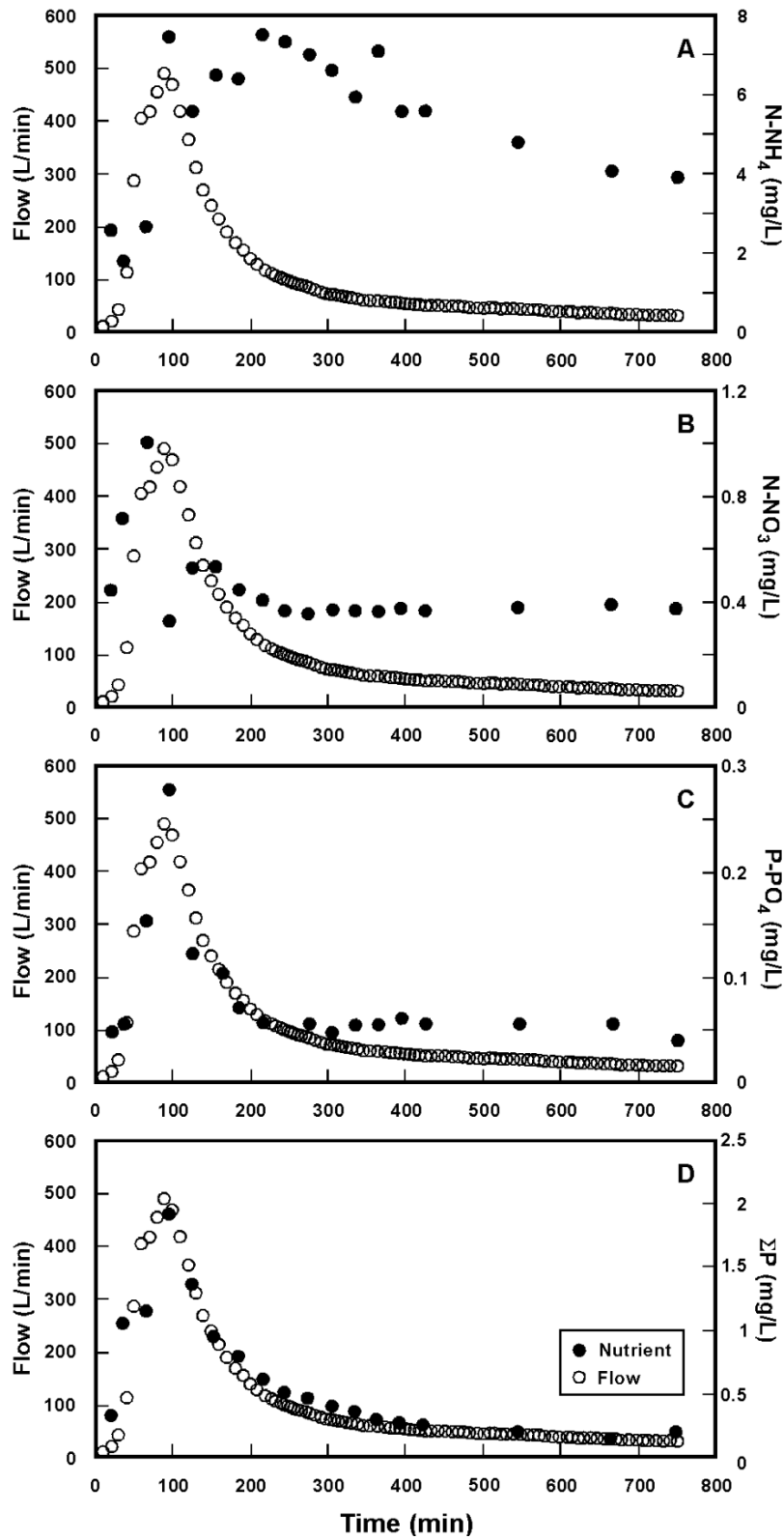


Figure 7: Graph showing flow (L/min) and concentration (mg/L) for each nutrient over duration of the 30-31 May 2018 storm event. A. N as dissolved ammonium (N-NH₄); B. N as dissolved nitrate (N-NO₃); C. P as dissolved orthophosphate (P-PO₄); and D as total phosphorus (ΣP).

Using the smooth curves generated by the cubic spline function, we estimate the total volume of the storm event, as well as the nutrient export of each nutrient species. For all six storm events, we calculated total nutrient export for each species (kg) and total flow volume (L) (Table 1). We observed the highest nutrient export values for all nutrients during the storm of 6-7 July with the lowest export during 20 June.

Rainfall Dates	Total Water Volume (liters)	P-PO ₄ (kg)	[ΣP] (kg)	N-NH ₄ (kg)	N-NO ₃ (kg)	Sum Dissolved N (kg)
30 -31 May 2018	82262	0.01	0.08	0.46	0.04	0.50
31 May - 1 June 2018	1667616	0.66	1.74	1.64	0.82	2.46
11 -12 June 2018	2392440	0.60	2.54	1.53	1.75	3.28
13 - 14 June 2018	3003349	0.83	1.25	0.00	2.54	2.54
20 June 2018	117022	0.02	0.07	0.09	0.10	0.19
6 - 7 July 2018	2856876	4.1	11.3	3.25	1.73	4.99
SUM	10119565	6.2	17.0	7.0	7.0	14.0
% Nutrient		20	54.8	22.6	22.6	

Table 1: Total water volume (L) and nutrient export (kg) for each measured storm event in the 2018 field season. Total water volume and total nutrient transport for each nutrient are shown for the 2018 season in the “SUM” row. The “% Nutrient” row shows the percentage of each nutrient exported during the storm events based on the total nutrient export of approximately 31 kg (ΣP + N-NH₄ + N-NO₃).

DISCUSSION

The overall intent of the project is to compare nutrient export before and to that after remediation efforts are in place. In addition, estimated nutrient export values during rain events must be put in context compared to nutrient export during fair-weather times in order to estimate annual nutrient export.

Base Flow versus Storm Nutrient Export

Baseflow export of nutrients should be much smaller than nutrient export during rainfall and storm events. Table 2 and Figure 8 show the statistical parameters of concentration values of each nutrient species from the BRC watershed during 2016, 2017, and 2018 (Evans et al., 2017; Buskirk et al., 2017; Winter et al., 2018, Buskirk et al., 2018). The median concentration values for ammonium, nitrate, phosphate and total phosphorous were 0.34, 0.5, 0.05, and 0.44 mg/L, respectively (Table 2). Multiplying the lowest measurable discharge rate of 30 L/min with these median concentration values over a period of 30 days yields an estimate of export for each nutrient species (Table 2).

Statistical Parameter	Nutrient Species			
	[N-NH ₄] (mg/L)	[N-NO ₃] (mg/L)	[P-PO ₄] (mg/L)	[P - ΣP] (mg/L)
N	244	224	232	135
Low	0	0	0	0
High	21.6	7.1	5.5	5.5
Median	0.3	0.5	0.1	0.4
Mean	2.6	0.9	0.3	1.4
Standard deviation	4.8	1.1	0.5	2.2
10th percentile	> 0	> 0	> 0	> 0
25th percentile	> 0	0.1	> 0	0.2
75th percentile	2.7	1.4	0.3	1.8
90th percentile	9.3	2.3	0.9	3.9
30-day export estimate (kg)	0.44	0.65	0.06	0.57

Table 2: Statistical parameters of baseflow concentration for each nutrient species from the BRC watershed. Data from Evans et al. (2017), Buskirk et al. (2017), Winter et al. (2018) and Buskirk et al. (2018).

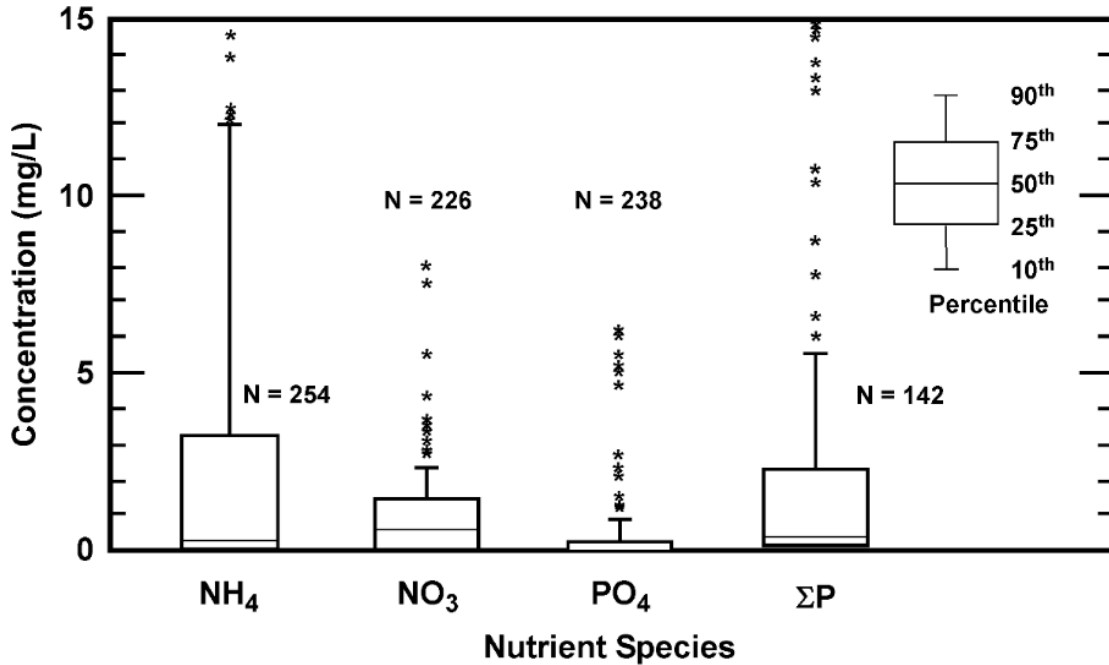


Figure 8: Box-and-whisker plot of concentration values for each nutrient species during the field seasons of 2016, 2017, and 2018 from the BRC watershed. Note the key showing the positions of each percentile value; asterisks are outlier values in excess of the 90th percentile.

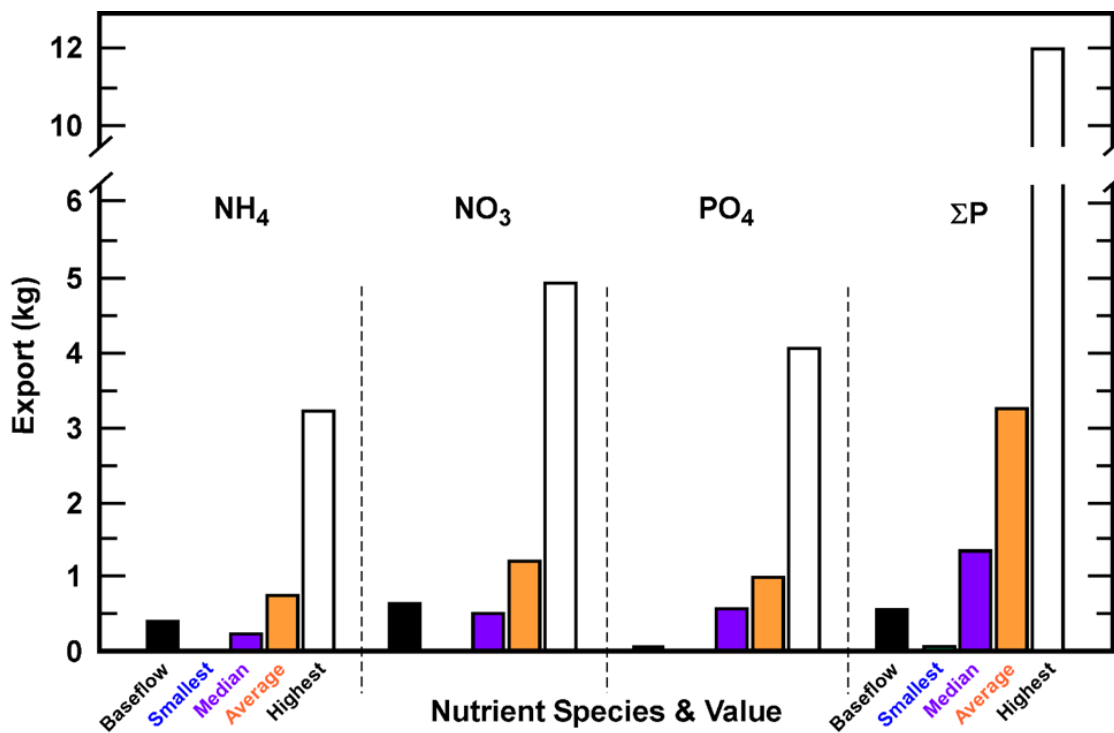


Figure 9. Graph comparing nutrient export of each nutrient species during baseflow (black columns) over a period of 30 days to the smallest (blue), median (purple), average (orange), and highest values (white) of nutrient export during rain events that typically occur for one to several days.

Most nutrient export occurs during rain events with baseflow transporting much smaller amounts of each nutrient species. To highlight the low significance of baseflow transport, Figure 9 compares baseline nutrient export of a period of 30 days compared to export of each nutrient species with the lowest, median, average, and highest values during rainfall events. Baseflow export is generally so low that the transport period must be lengthened considerably to 30 days to register on the graph. Baseflow export is typically ~22 to 25 times less than median values based on one day of discharge. This indicates that baseflow nutrient transport can be considered negligible relative to rainfall export.

Relationship between Flow Volume and Nutrient Export

In order to compare nutrient export values before remediation to those afterward, annual nutrient export must be estimated in both scenarios. If there is a reasonable mathematical relationship between flow volume and nutrient export, nutrient export can then be estimated for every storm event because hydrograph data is always collected to calculate flow volume. Collective estimates of nutrient export for every rainfall event will yield annual export values for each nutrient species.

We plotted graphs of nutrient export for each species against total water volume for every recorded storm event (Figure 10). Generally, as flow volume increases, total nutrient export also increases. When total water volume is at or near zero, nutrient export is proportionally low as well, showing that nutrient export is negligible between rain events when water volume is low. However, these relationships are not observed with ammonium, which shows no apparent correlation between water volume and nutrient export.

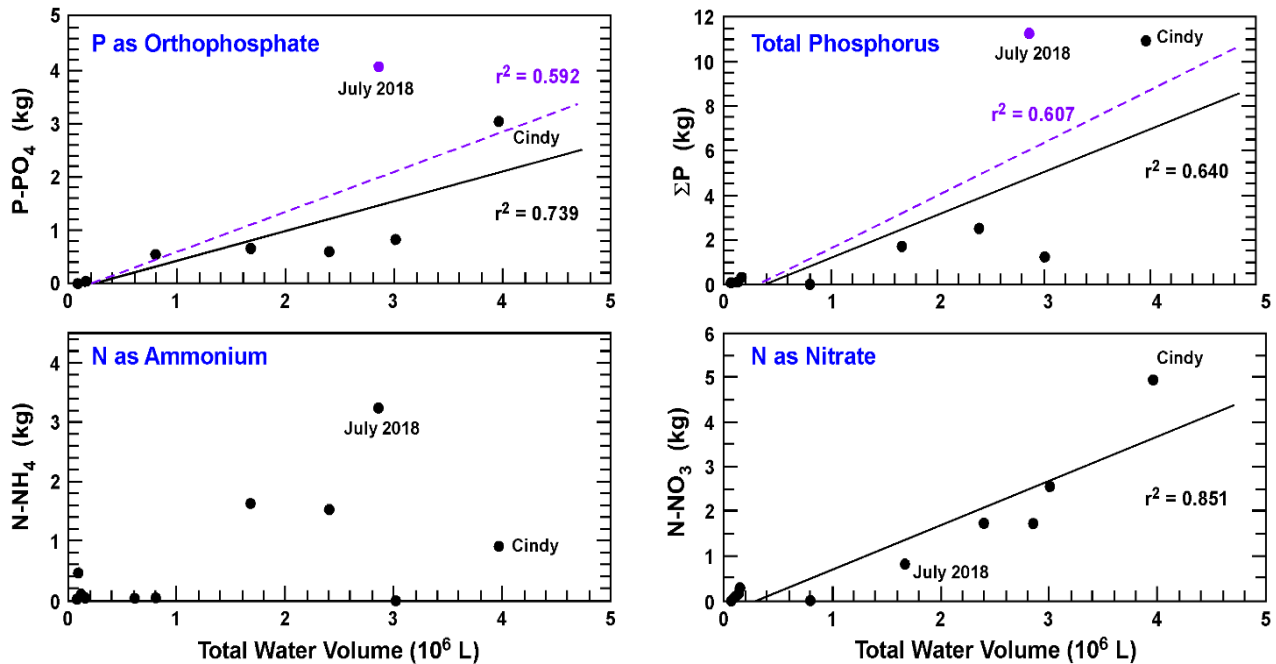


Figure 10: Plots of nutrient export values (kg) for each nutrient species versus total water volume (L) for all measured storm events of 2017 and 2018. The solid line in each plot shows the best line fit results and correlation coefficient (r^2) for all storms excepting that of 6-7 July 2018, which is an outlier for P-PO₄ and ΣP . The dashed line includes the data for 6-7 July 2018 with the r^2 value.

We test for a mathematical relationship between total storm volume and nutrient export (Borowski et al., 2018). Nitrate shows the strongest linear relationship, with a correlation coefficient (r^2 value) of 0.851, but any linear response is weaker for dissolved orthophosphate and total phosphorus. For these species, results from the 6-7 July 2018 storm is an outlier. Not including the 6-7 July data, there is a potential linear relationship between flow volume and nutrient export with a correlation coefficient of 0.739 for orthophosphate and 0.640 for total phosphorus (solid lines in Figure 9). Any linear relationship degrades when the data for the July storm are included.

The lack of a strong mathematical relationship between nutrient export and storm volume makes annual estimation of nutrient export problematical. Therefore, Clemons et al. (2019) investigated the relationship of nutrient export to other pertinent parameters (rainfall amount,

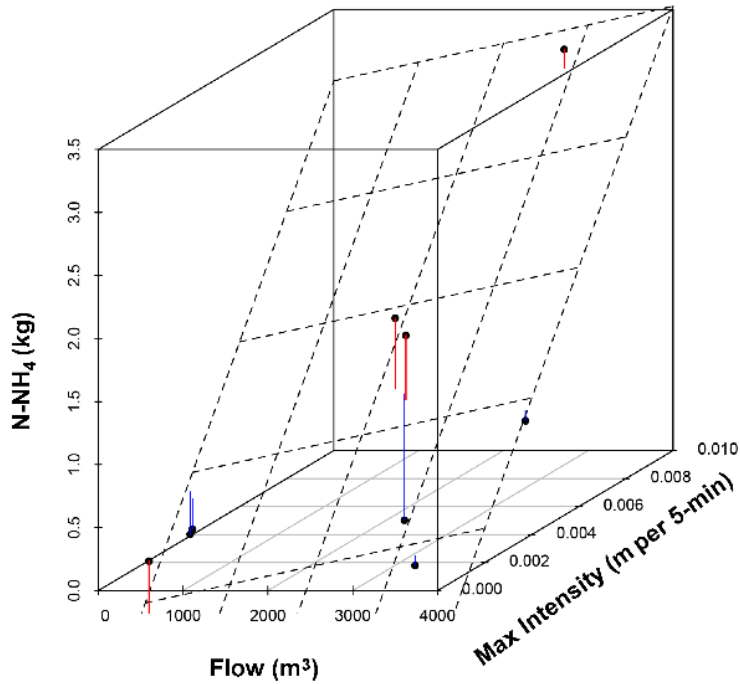


Figure 11: A. Three-dimensional plot of NH₄ export, total flow volume, and maximum rainfall intensity. After Clemons et al., 2019.

rainfall intensity, rain duration, and time between rainfall events), finding significant multi-variable relationships with each nutrient. For example, ammonium was found to have the strongest relationship with maximum rainfall intensity and flow with a r^2 value of 0.797 (Figure 11), revealing a significant correlation where none existed with flow volume alone. Nitrate has the best relationship with rainfall amount and flow ($r^2 = 0.653$), whereas phosphate is most strongly correlated ($r^2 = 0.758$) with maximum rainfall intensity and flow (Clemons et al., 2019).

Next Steps

The next step in this research is to solidify the relationship of nutrient export to discharge and rainfall parameters to estimate nutrient export annually. Once annual nutrient export can be accurately estimated, mitigation techniques can be effectively evaluated on the Farm. Using

annual estimates will allow us to compare overall nutrient loads before and after mitigation efforts.

SUMMARY

We investigated the export of dissolved nitrogen (ammonium, NH_4^+ ; nitrate, NO_3^-), dissolved phosphorus (orthophosphate, PO_4^{3-}), and total phosphorus (ΣP) from Meadowbrook farm in Madison County, Kentucky. We used an instrumented weir to measure discharge and an autosampler to collect water during rain events to measure nutrient concentration.

During the 2018 field season, we successfully measured flow and nutrient concentrations for six storm events. Of these events, the largest total water volume and nutrient loads occurred during the 6-7 July storm. During this storm, total water volume was over 2.8 million liters with nutrient export of 4.1 kg of P- PO_4 ; 11.3 kg of total phosphorus; 3.3 kg of N- NH_4 ; and 1.7 kg of N- NO_3 [5 kg N].

Most nutrients followed a roughly linear trend of increasing nutrient export with increasing total storm volume. However, this is not the case with ammonium, whose relationship with flow is apparently random. For orthophosphate and total phosphorus, the 6-7 July storm is a substantial outlier when compared to the rest of the data, so that any linear relationship between flow and export is not robust enough to estimate nutrient export in the absence of concentration data. However, other parameters like rainfall amount and rainfall intensity show closer mathematical relationships to nutrient export than discharge alone.

The next step in the project is to establish better estimates of nutrient export using flow data and key rainfall parameters. Then nutrient export for each rainfall event can be estimated to calculate annual nutrient export. With these estimates, nutrient mediation efforts at the Farm can be properly evaluated.

REFERENCES

- Allaire S.E., C. Sylvain, S.F. Lange, G. Thériault, P. Lafrance, 2015. Potential efficiency of riparian vegetated buffer strips in intercepting soluble compounds in the presence of subsurface preferential flows. *PLoS ONE*, 10(7): e0131840.
- Arbuckle, K.E., J.A. Downing, 2001. The influence of watershed land use on lake N: P in a predominantly agricultural landscape. *Association for the Sciences of Limnology and Oceanography*, v. 46, p. 970-975.
- Baker, L.A., 1992, Introduction to nonpoint source pollution in the United States and prospects for wetland use. *Ecological Engineering*, n. 1, p. 1-26.
- Blinn C.R., M.A. Kilgore, 2001. Riparian management practices: A summary of state guidelines. *Journal of Forestry*, v. 99, n. 8, p. 11-17.
- Borowski, W.S., J.M. Malzone, J.S. Winter, R.M Penn, R.E. Buskirk, 2018. Quantifying nutrient export from an upland, intermittent stream draining a working farm, Madison County, Kentucky: Prelude to nutrient mitigation. *Geological Society of America annual conference*, November, 2018.
- Buskirk, R.E., W.S. Borowski, and J.M. Malzone, 2018. Characterization of groundwater and surface water geochemistry in an agricultural setting at ECU Meadowbrook Farm, Madison County, Kentucky. Kentucky Water Resources Research Institute (KWRI) Symposium, 19 March 2018, *Proceedings*, pg. 70-71.
- Buskirk, R.E., H.R. Evans, W.S. Borowski, J.M. Malzone, 2017. Nutrient contamination from non-point sources: Dissolved nitrate and ammonium in surface and subsurface waters at ECU Meadowbrook Farm, Madison County, Kentucky. *GSA Abstracts with Program*, 49(2), doi:10.1130/abs/2017NE-290271.
- Carpenter, S.R., N.F. Caraco, D.L. Correll, R.W. Howarth, A.N. Sharpley, V.H. Smith, 1998. Nonpoint pollution of surface waters with phosphorus and nitrogen. *Ecological Applications*, v. 8, n. 3, p. 559-568.
- Clemons, Trevor, J.M. Malzone, R. Penn, W.S. Borowski, 2019. How does drought length impact the runoff and nutrient storm response in an agricultural, intermittent catchment in Central Kentucky? *Annual Symposium, Kentucky Water Resources Research Institute (KWRI)*, March 25, 2019.
- Cooke, S.E., E.E. Prepas, 1998. Stream phosphorus and nitrogen export from agricultural and forested watersheds on the Boreal Plain. *Canadian Journal of Fisheries and Aquatic Sciences*, v. 55, n. 10, p. 2292-2299.
- Diaz, R.J., R. Rosenberg, 2008. Spreading dead zones and consequences for marine ecosystems. *Science*, v. 321, n. 5891, p. 926-929.

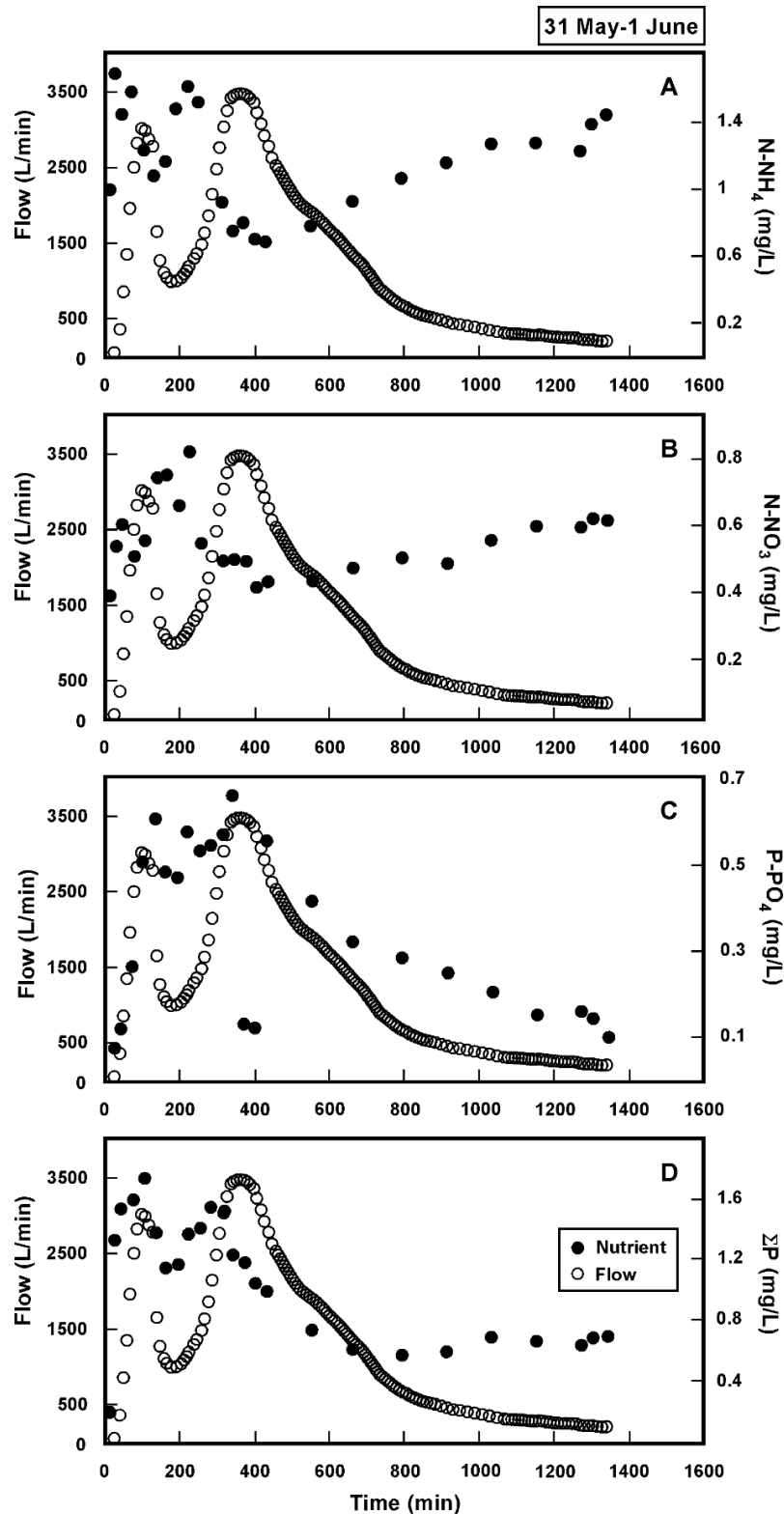
- Dodds, W.K., 2006. Nutrients and the “dead zone”: The link between nutrient ratios and dissolved oxygen in the northern Gulf of Mexico. *Frontiers in Ecology and the Environment*, v. 4, n. 4, p. 211-217.
- Doolittle, P. 2014. Ascorbic acid method for phosphorus determination. Unpublished lab manual excerpt.
- Dubrovsky, N.H., K.R. Burow, G.M. Clark, J.A.M. Gronberg, P.A. Hamilton, K.J. Hitt, D.K. Mueller, M.D. Munn, B.T. Nolan, L.J. Puckett, M.G. Rupert, T.M. Short, N.E. Spahr, L.A. Sprague, W.G. Wilber, 2010. The quality of our Nation’s waters—nutrients in the Nation’s streams and groundwater, 1992–2004: *U.S. Geological Survey Circular 1350*, 174 p.
- Echevarria, C., L. Wilson, W.S. Borowski, 2017. Sources of nutrient pollution from the ECU Meadowbrook Farm, Madison County, Kentucky. *McNair Scholars Conference*, University of Buffalo, 28 July 2017.
- Evans, H.R., R.E. Buskirk, W.S. Borowski, J.M. Malzone, 2017. Nutrient contamination from non-point sources: Dissolved phosphate in surface and subsurface waters at ECU Meadowbrook Farm, Madison County, Kentucky. *GSA Abstracts with Program*, 49(2), doi:10.1130/abs/2017NE-290273.
- Gharabaghi, B., R.P. Rudra, P.K. Goel, 2006. Effectiveness of vegetative filter strips in removal of sediments from overland flow. *Water Quality Research Journal of Canada*, v. 41, n. 3, p. 275–282.
- Gieskes, J.M., T. Gamo, H. Brumsack, 1991. Chemical methods for interstitial water analysis aboard JOIDS Resolution. *ODP Technical Note 15*, 60 pp.
- Guang, J., T.J. Bierma, 2018. Phosphorus recovery from surface waters: Protecting public health and closing the nutrient cycle. *Journal of Environmental Health*, v. 81, n. 2, p. 16–22.
- Hoorbeek, J.A., 2011. Water pollution policies and the American states: Runaway bureaucracies or congressional control? State University of New York Press, 2011, ISBN 978-1-4384-3541-1.
- Ji, L., L. Zheng, L. Yajiao, L. Peng, J. Chunbo, 2018. Experimental study and simulation of phosphorus purification effects of bioretention systems on urban surface runoff. *PLoS ONE*, 13(5): e0196339.
- Jordan, T.E., D.L. Correll, D.E. Weller, 1997. Nonpoint source discharges of nutrients from Piedmont watersheds of Chesapeake Bay. *Journal of the American Water Resources Association*, v. 33, n. 3, p. 631–645.

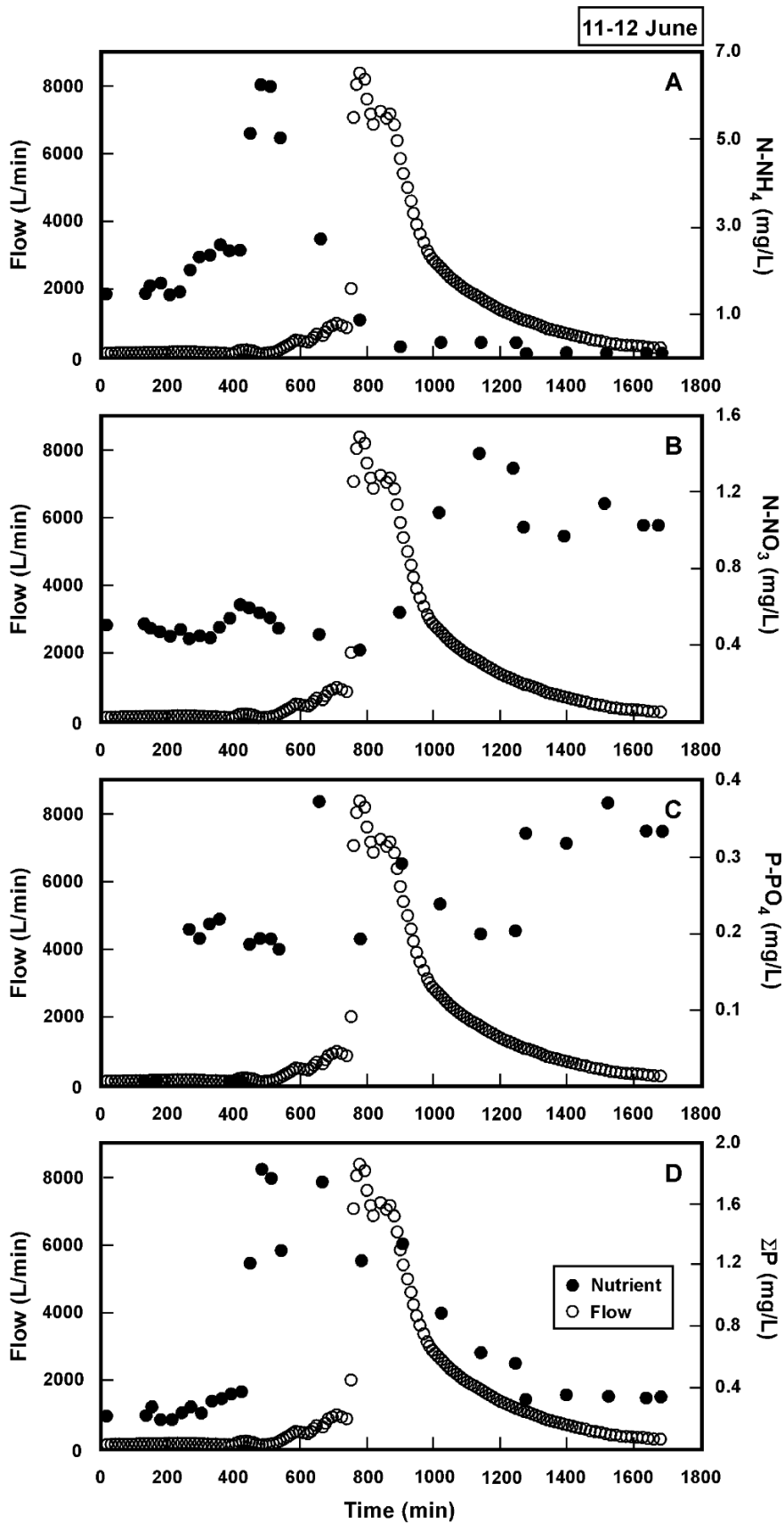
- Kelley, L., H.R. Evans, R.E. Buskirk, J.M. Malzone, and W.S. Borowski. 2017. Groundwater and subsurface water in a landscape with shallow bedrock: Implications for agricultural nutrient export. *GSA Abstracts Program*, 49(2), 49, No. 2, doi: 10.1130/abs/2017NE-290530.
- Kentucky Mesonet, data for Madison County, Station 64. Available at http://www.kymesonet.org/historical_data.php.
- Moltz, H.L.N., W. Rast, V. Lopes, S. Ventura, 2011. Use of spatial surrogates to assess the potential for non-point source pollution in large watersheds. *Lakes & Reservoirs: Research & Management*, v. 16, n. 1, p. 3-13.
- National Research Council (U.S.), 2000. Clean coastal waters: Understanding and reducing the effects of nutrient pollution. *National Academies Press*, retrieved from <http://search.ebscohost.com/login.aspx?direct=true&AuthType=ip,shib&db=nlebk&AN=46031&site=eds-live&scope=site>.
- Neary, D.G., W.T. Swank., and H. Riekerk., 1989. An overview of nonpoint source pollution in the southern United States. *General technical report SE - U.S. Department of Agriculture, Forest Service, Southeastern Forest Experiment Station (USA)*, ISSN 0887 4859.
- Pinckney, J.L., H.W. Paerl, P. Tester, T.L. Richardson, 2001. The role of nutrient loading and eutrophication in estuarine ecology, *Environmental Health Perspectives*, v. 109, p. 699-706
- Rabalais, N.N., R.E. Turner, W.J. Wiseman Jr., 2002. Gulf of Mexico Hypoxia, A.K.A. “The Dead Zone”. *Annual Review of Ecology and Systematics*, V. 33, p. 235-263.
- Smith, V.H., G.D. Tilman, J.C. Nekola, 1999. Eutrophication: Impacts of excess nutrient inputs on freshwater, marine, and terrestrial ecosystems. *Environmental Pollution*, v. 100, p. 179-196.
- Solorzano, L., 1969. Determination of ammonia in natural water ways by phenol-hypochlorite method. *Limnology Oceanography*, 14:799-801.
- SRS1 Cubic Spline for Excel, 2015. *SRS1 Software, LLC*. Retrieved from <http://www.srs1software.com/SRS1CubicSplineForExcel.aspx>
- Strickland, J.D.H., T.R. Parsons., 1968. A manual for sea water analysis. *Bull Fisheries Research Board Canada*, 167.
- Strokal, M., L. Ma, Z. Bai, S. Luan, C. Kroeze, O. Oenema, G. Velthof, F. Zhang, 2016. Alarming nutrient pollution of Chinese rivers as a result of agricultural transitions. *Environmental Research Letters*, v. 11, 024014.

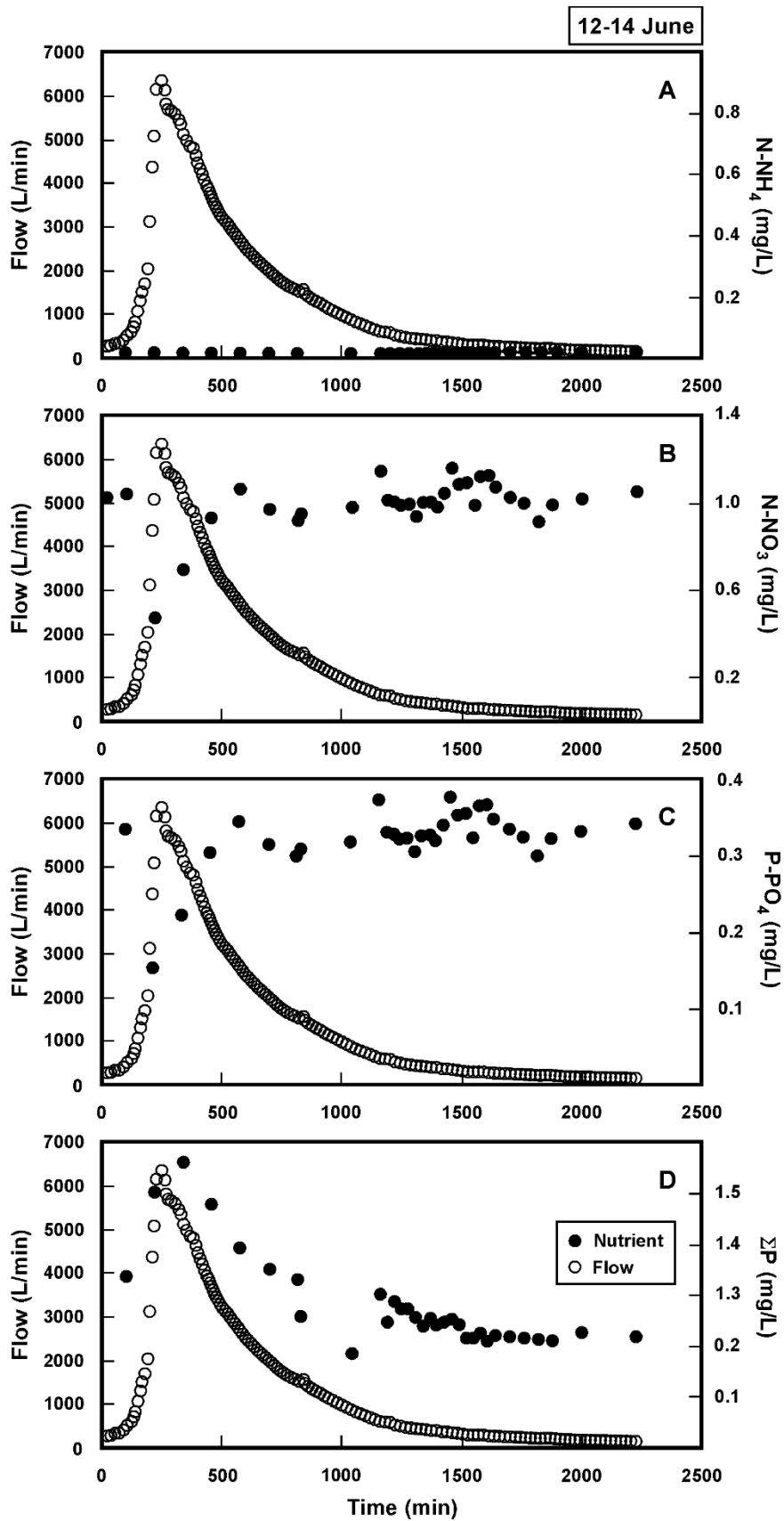
- Vanni, M.J., W.H. Renwick, J.L. Headworth, J.D. Auch, M.D. Schaus, 2001. Dissolved and particulate nutrient flux from three adjacent agricultural watersheds: A five-year study. *Biogeochemistry*, v. 54, n. 1, p. 85-114.
- Winter, J.S., W.S. Borowski, and J.M. Malzone, 2018. Nutrient export from a proximal intermittent stream draining ECU Meadowbrook Farm, Madison County, Kentucky. Kentucky Water Resources Research Institute (KWRI) Symposium, 19 March 2018, *Proceedings*, pg. 72-73.
- Zhang X., X. Liu, M. Zhang, R.A. Dahlgren, 2010. A review of vegetated buffers and a meta-analysis of their mitigation efficacy in reducing nonpoint source pollution. *Journal of Environmental Quality*, v. 39, n. 1, p. 76-84.

APPENDIX

Figure A1: Graphs showing flow (L/min) and concentration (mg/L) for each nutrient over duration each 2018 storm event (excluding 30-31 May; see Figure 7). A. N as dissolved ammonium (N-NH₄); B. N as dissolved nitrate (N-NO₃); C. P as dissolved orthophosphate (P-PO₄); and D. as total phosphorus (ΣP).







20 June

